Eur. J. Mineral.
2016, **28**, 495–505
Published online 5 January 2016

Cairncrossite, a new Ca-Sr (-Na) phyllosilicate from the Wessels Mine, Kalahari Manganese Field, South Africa

GERALD GIESTER[1,*], CHRISTIAN L. LENGAUER[1], HELMUT PRISTACZ[1], BRANKO RIECK[1], DAN TOPA[2] and KARL-LUDWIG VON BEZING[3]

[1] Institut für Mineralogie und Kristallographie, Universität Wien, Althanstr. 14, 1090 Wien, Austria
*Corresponding author, e-mail: gerald.giester@univie.ac.at
[2] Zentrale Forschungslaboratorien, Naturhistorisches Museum, Burgring 7, 1010 Wien, Austria
[3] Wolseley Street 19, Kimberley 8301, South Africa

Abstract: Cairncrossite is a new phyllosilicate species found in manganese ore on dumps of the Wessels Mine, Kalahari Manganese Field, South Africa. Associated minerals are richterite, sugilite, lizardite and fibrous pectolite. It occurs as radiating platy micaceous aggregates of up to 1 cm in size. Cairncrossite is colourless, appearing white, and the crystals are translucent to transparent with a white streak and vitreous to pearly lustre. The crystals are sectile before brittle fracture, with a Mohs hardness of 3. A perfect cleavage parallel (001) is observed. The calculated density is 2.486 g cm^{-3}. The mineral is biaxial positive with $n_\alpha = 1.518(2)$, $n_\beta = 1.522(2)$, $n_\gamma = 1.546(2)$, $2V_{obs} = 33.9(6)^\circ$ ($2V_{calc} = 44.97^\circ$) at 589.3 nm and 24°C. The orientation of the indicatrix is Z ^ **c*** $= 10^\circ$. The dispersion is weak ($r < v$) and no pleochroism is observed. An intense light-blue fluorescence is emitted under shortwave UV radiation. Cairncrossite is triclinic, space group $P\overline{1}$, $a = 9.6265(5)$, $b = 9.6391(5)$, $c = 15.6534(10)$ Å, $\alpha = 100.89(1)$, $\beta = 91.27(1)$, $\gamma = 119.73(1)^\circ$, $V = 1227.08(13)$ Å^3, $Z = 1$. The strongest lines in the Gandolfi X-ray powder-diffraction pattern [*d* in Å(*I*)(*hkl*)] are 15.230 (100)(001), 8.290 (15)(1–10), 5.080(25)(003), 3.807(30)(004), and 3.045(20)(005). The chemical composition obtained by electron-microprobe analysis is Na_2O 3.06, K_2O 0.11, CaO 18.61, SiO_2 54.91, SrO 11.75, total 88.44 wt%. The relevant empirical formula, based on 16 Si atoms per formula unit (*apfu*) and TGA data is: $Sr_{1.99}K_{0.02}Ca_{5.81}Na_{1.73}\,Si_{16}O_{55.84}H_{30.33}$. Taking variable sodium contents into account, the idealized structural formula is $Sr_2Ca_{7-x}Na_{2x}(Si_4O_{10})_4(OH)_2(H_2O)_{15-x}$ with $0 \leq x \leq 1$, and the simplified formula for sodium-rich crystals is $SrCa_3Na(Si_4O_{10})_2(OH)(H_2O)_7$ with $Z = 2$. The structure of cairncrossite was refined on single-crystal X-ray data (Mo$K\alpha$ radiation) to $R1 = 0.047$. Cairncrossite belongs to the gyrolite and reyerite mineral groups, it is characterized by sheets consisting of edge-sharing CaO_6 octahedra, which are corner-linked on both sides to silicate layers. These units are intercalated by layers formed by SrO_8 polyhedra, which are arranged in pairs via a common edge, and further bound to disordered NaO_6 polyhedra. A complex system of hydrogen bonds strengthens the linkage to adjacent silicate layers. Cairncrossite exhibits a two-phase endothermic weight loss of the H_2O molecules in the range 25–400°C; however, the mineral shows a nearly complete rehydration capability up to 400°C. The new mineral is named in honour of Bruce Cairncross, Professor and Head of the Department of Geology, University of Johannesburg.

Key-words: cairncrossite; new mineral; crystal structure; phyllosilicate; calcium strontium sodium silicate hydroxyl hydrate; Wessels Mine; Kalahari Manganese Field.

Introduction

Early in 1988 one of the authors (KLvB) collected a specimen of a white micaceous mineral in manganese ore on dumps of the Wessels Mine, Kalahari Manganese Field, Northern Cape Province, South Africa. Only one specimen was found. According to the mine captain the ore came from Block 17 of the Wessels Mine. Initial analysis by Roger Dixon, Univ. of Pretoria, suggested it to be a new mineral but no further investigations were done. The results of the present study first indicated it to be a new strontium-calcium-sheet-silicate, with an idealized formula $Sr_2Ca_7(Si_4O_{10})_4(OH)_2(H_2O)_{15}$, belonging to the gyrolite–reyerite mineral group. After acceptance of cairncrossite by the CNMMN in early 2013, further parts of the original sample material became available to one of the authors (GG), allowing more detailed single-crystal X-ray measurements as well as extended studies on chemical composition, crystal chemistry and thermal properties. It became evident that cairncrossite exhibits a variable chemical composition with chemical zoning, and should better be described as $Sr_2Ca_{7-x}Na_{2x}(Si_4O_{10})_4(OH)_2(H_2O)_{15-x}$ with x in the range 0–1. Cairncrossite joins the group of new silicate species from the Kalahari Manganese Field investigated up to now by the authors, like effenbergerite, $BaCuSi_4O_{10}$ (Giester & Rieck, 1994), wesselsite, $SrCuSi_4O_{10}$ (Giester & Rieck, 1996), and colinowensite, $BaCuSi_2O_6$ (Rieck *et al.*, 2015). A preliminary note on the

DOI: 10.1127/ejm/2016/0028-2519
0935-1221/16/0028-2519 $ 4.95

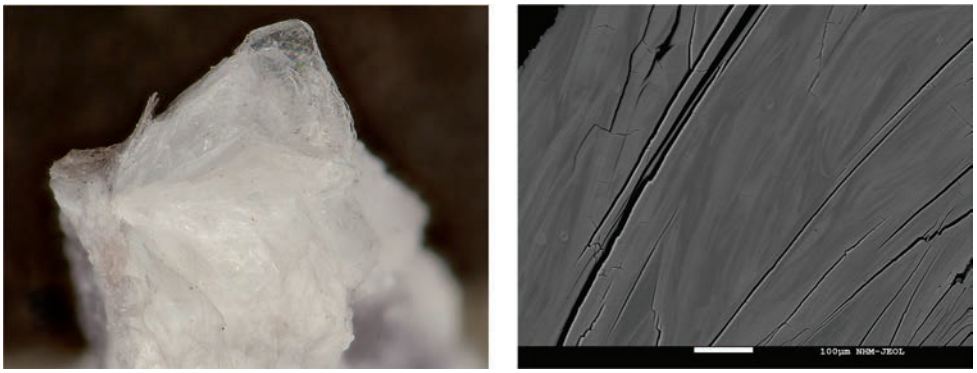

Fig. 1. (a) Photograph of cairncrossite. Field of view: 5mm. (b) High-contrast back-scattered electron image of the polished sample used for chemical analysis.

thermal behaviour of cairncrossite has already been presented at the MinPet2013 meeting (Pristacz *et al*., 2013).

Mineral name and type material

The mineral is named cairncrossite in honour of Bruce Cairncross, Professor and Head of the Department of Geology, University of Johannesburg. He is author of several books and numerous articles on the mineralogy of the Southern African Region with special interest in the Kalahari Manganese Field. He has contributed significantly towards awareness of diversity of the mineralogy in Southern Africa.

The new mineral has been approved by the Commission on New Minerals, Nomenclature and Classification of the International Mineralogical Association under number IMA 2013–12. Holotype material has been deposited in the collections of the Institute for Mineralogy and Crystallography at the University of Vienna (inventory number 13079) and the collection of the Museum of Natural History of Vienna (inventory number N 9858).

Occurrence

Cairncrossite was found lining the central cavity of a vug in manganese ore that came from Block 17 of the Wessels Mine, Kalahari Manganese Field, Northern Cape Province, South Africa. Associated minerals include blue manganoan richterite, minor manganoan sugilite, minor grey to orange lizardite and fibrous pectolite, the latter as small crystals lining secondary cavities. Cairncrossite is the last mineral to have formed during metasomatic alteration of a primary carbonate-rich manganese ore.

Appearance, physical and optical properties

Cairncrossite is colourless, appearing white, and the crystals are translucent to transparent with a white streak. The lustre is vitreous to pearly. The crystals form densely packed, radiating platy micaceous aggregates up to 1 cm in size (Fig. 1a), which closely resemble brucite $Mg(OH)_2$ also reported from the Kalahari Manganese fields (N'chwaning Mine: see von Bezing *et al.*, 1991). The crystals are sectile before brittle fracture, with a Mohs hardness of 3. A perfect cleavage parallel (001) is observed. The density is 2.50(3) g.cm^{-3} on the basis of buoyancy measurements with a microbalance. This value is in good accordance with the calculated density of 2.486 g. cm^{-3} derived from chemistry and crystal-structure data.

A cairncrossite platelet was mounted on glass fibre and inspected under a polarizing microscope equipped with a spindle stage and using Cargille refractive index liquids ($\Delta n = 0.002$). Optical angle ($2V_{obs} = 33.9(6)^\circ$) and orientation of the optical axes were derived from extinction data using the software EXCALIBR II (Bartelmehs *et al*., 1992). The mineral is biaxial positive with $n_\alpha = 1.518(2)$, $n_\beta = 1.522(2)$, $n_\gamma = 1.546(2)$, $2V_{calc} = 44.97^\circ$ at 589.3 nm and 24°C. The acute bisectrix Z is about 10° from perpendicular to {001} (**c***). The dispersion is weak ($r < v$) and no pleochroism is observed. Intense light-blue fluorescence is emitted under shortwave UV light. Calculating K_c for the empirical formula of cairncrossite with x = 1 using the Gladstone-Dale relationship (Gladstone & Dale, 1863) with the values given by Mandarino (1976) revealed an averaged refractive index of $n = 1.548$. The compatibility index resulted in 0.036, which is rated as excellent (Mandarino, 1981).

Chemical composition

Chemical analyses (15) of a first sample (three grains) were carried out in 2012 using an electron microprobe (wavelength dispersive spectrometry (WDS) mode, 20 kV, 20 nA, *ca.* 6 µm beam diameter) and led to the formula $Sr_2Ca_7(Si_4O_{10})_4(OH)_2(H_2O)_{15}$ with minor amounts of Mg and Al. Subsequently, it was noticed that cairncrossite showed a variable chemical composition with evidence of zoning and may also incorporate sodium. The rims of the platelets occasionally are significantly depleted in sodium. In 2014, analytical data for Sr, Ca, Na, Mg, Si

and Al were obtained from the AAF's (the Austrian Armed Forces ChemLab) newly commissioned JEOL JXA-8230 SuperProbe which has integrated dual-crystal wavelength dispersive spectrometers and an energy dispersive detector. The highly automated system allowed the acquisition of 194 point measurements distributed over 31 grains (*ca.* 200x50x5 μm^3), all under the same operating conditions (20 kV, 20 nA, *ca.* 4 µm beam diameter). The results revealed different domains within the same sample (but not the same grain): some containing higher amounts of Na (mean value of 2.90 wt% Na_2O for 78 spots) and some containing only traces of Na (mean value of 0.22 wt% Na_2O, 116 spots).

In 2015, further chemical analyses were performed at the NHM, Vienna, Austria, on a JEOL Hyperprobe JXA-8530F instrument, operated in WDS mode, at 15 kV, 20 nA and defocused beam diameter of 30 µm, under the control of *Probe for EMPA* package of programs. Standards and lines used were: Na*Kα* (NaCl), Si *Kα* (olivine), K*Kα* (KCl), Ca*Kα* (wollastonite) and Sr*Lα* (celestine). Other elements (Al, Mg, Ti, Cr, Mn, Fe and Ni) were sought, but not detected. Fourteen analyses of one aggregate gave as an average (range): Na_2O 3.06 (2.48–3.15), K_2O 0.11 (0.09–0.12), CaO 18.61 (18.17–19.24), SiO_2 54.91 (53.20–55.85), SrO 11.75 (11.25–12.11), total 88.44 (86.32–89.97) wt%.

The empirical formula, calculated on the basis of 16 Si *apfu* (according to structure refinement, $Z = 1$, see below) and the H_2O content deduced from observed TGA loss (∼15 wt%), is $Sr_{1.99}K_{0.02}Ca_{5.81}Na_{1.73}\ Si_{16}O_{55.84}H_{30.33}$. Using the simplified formula (x = 1, with $Z = 2$) $SrCa_3Na(Si_4O_{10})_2(OH)(H_2O)_7$ for the sodium-rich crystal fragment studied by single-crystal X-ray analysis, the ideal, theoretical, elemental composition can be calculated as: Sr 9.538, Ca 13.089, Si 24.458, Na 2.503, O 48.767 and H 1.646 wt%, or, expressed in oxide wt%: SrO 11.280, CaO 18.314, SiO_2 52.325, Na_2O 3.373, H_2O 14.708, sum 100 wt%. The slight discrepancy between empirical and simplified structural formula is believed to be (an artefact) due to the high H_2O content and implicit high sensitivity of the polished surface under defocused beam (Fig. 1b). Taking variable amounts of sodium into account, the formula of cairncrossite may be given as $Sr_2Ca_{7-x}(Na, Ca_{0.5})_{2x}(Si_4O_{10})_4(OH)_2(H_2O)_{15-x}$ ($0 \leq x \leq 1$).

Thermal analyses

For the thermogravimetry (TG) and differential scanning calorimetry (DSC) of cairncrossite several samples of 19–21 mg of carefully ground material were loaded to 70 µl Al_2O_3 crucibles. The measurements were performed on a Mettler-Toledo TGA/SDTA851 thermo balance from 25 to 1100°C with a heating rate of 5°C.min^{-1} and N_2 flow of 25 ml.min^{-1} as purge gas (Messer 5.0). For the DSC a Mettler-Toledo DSC821e equipped with a liquid-nitrogen cooling device, 40 µl Al crucibles without lids and sapphire as reference were used, applying a heating rate of 10°C.min^{-1} from –50 to 600°C and N_2 flow of 50 ml.min^{-1} for purge and dry gas (Messer 5.0). Prior to evaluation, data were corrected by blind curves measured before and after the sample measurement. For evaluation the Mettler-Toledo STAR^e software was used (Fig. 2).

All samples revealed the reproducible behaviour of a main weight loss from –9.0 to –9.2 wt% for 25 to 150°C

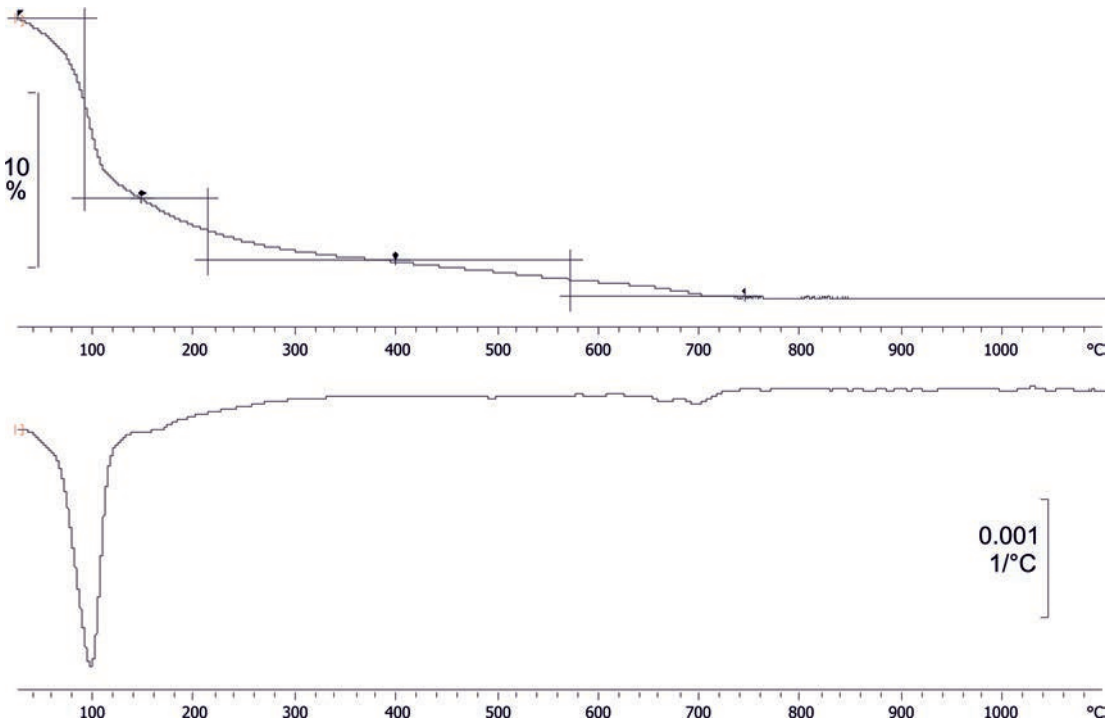

Fig. 2. Plot of the thermogravimetric data (TG upper curve) and their first derivative (DTG lower curve) for cairncrossite.

($DTG_{max} \approx 100°C$), followed by a second loss of –3.9 wt% up to 400°C ($DTG_{max} \approx 175°C$). After a thermal stability up to 500°C two further weight losses can be detected at 550°C (–1.2 wt%) and 700°C (–0.9 wt%). The DSC data proved the weight losses at 100, 175 and 550°C to be endothermal. The minor variability of the main weight loss values reflects the different hydration conditions, which can be expected for phyllosilicates. The most outstanding physico-chemical feature of cairncrossite, however, is an almost complete rehydration capability after heating to 400°C. The corresponding weight loss of ~ 13 wt% is in good agreement with the calculated water content (7 H_2O = 13.73 wt%) of the simplified formula. The calculated OH-content is equivalent to 0.98 wt%, which is close to the observed weight loss sum above 600°C. After heating dehydrated cairncrossite up to 600°C with partial dehydroxylation, no rehydration behaviour was observed.

Powder X-ray diffractometry

Due to the pronounced cleavage and platy habit parallel (001) and pronounced textured powder patterns (Fig. 3) the powder diffraction (PXRD) data for cairncrossite (Table 1) were obtained with a Gandolfi camera (Gandolfi, 1964) in asymmetric setting (Straumanis & Jevin, 1936) using Ni-filtered Cu$K\alpha$ radiation. Angular data were corrected for film shrinkage, intensities estimated visually, *hkl* assignments based on the theoretical intensities from the refined structure model (Kraus & Nolze, 1996), and the unit-cell parameters were obtained from least-squares refinement on 54 observed angular values (Holland & Redfern, 1997). The refined triclinic unit-cell parameters from these powder data are $a = 9.626(1)$, $b = 9.639(1)$, $c = 15.651(2)$ Å, $\alpha = 100.88(1)$, $\beta = 91.28(1)$, $\gamma = 119.72(2)°$ and $V = 1227.0(2)$ Å^3, which are similar to the results of the single-crystal data processing (Table 2). It is worth to note that the strongest lines of the PXRD pattern show a similarity to the data of the structurally unknown Ca-zeolite cowlesite (Wise & Tschernich, 1975).

According to the findings of the thermal analyses these TG products were investigated by laboratory powder diffractometry (Philips X'Pert, Cu$K\alpha$, graphite secondary monochromator, variable slit configuration, φ-spinning). After 24 h of equilibration at ambient conditions the sample materials were fixed with grease to a low-background silicon sample carrier. A comparison of the PXRD patterns is shown on Fig. 3. As expected from the physical properties the pattern of cairncrossite exhibits a pronounced texture with an almost perfect ordering parallel (001) as compared to a calculated powder pattern based on the parameters of the single-crystal investigations.

Concerning the results of the thermal analyses, which indicate almost complete rehydration after heat treatment below 400°C, the recoverability of cairncrossite is confirmed by these PXRD investigations. Whereas the PXRD patterns of raw and heat-treated materials are very comparable (Fig. 3), peak broadening indicates a decrease of the microstructural quality after the treatment. After heating to 600°C the structure collapses and sample material disintegrates into the layered arrangement of the K-phase, a CSH-phase similar to $Ca_7Si_{16}O_{38}(OH)_2$ (Gard *et al*., 1981). Enlargement of the *d* values of the strong basal reflections indicate a possible Sr substitution. Further heating of the K-phase leads to dehydroxylation and occurrence of α-$CaSiO_3$, pseudowollastonite (Yamanaka & Mori, 1981).

X-ray diffraction data and crystal-structure determination

Small fragments were carefully prepared for collecting single-crystal X-ray data at room temperature on a Kappa ApexII CCD diffractometer equipped with a CCD area detector and an Incoatec Microfocus Source IμS (30 W, multilayer mirror, Mo$K\alpha$). Several sets of phi- and

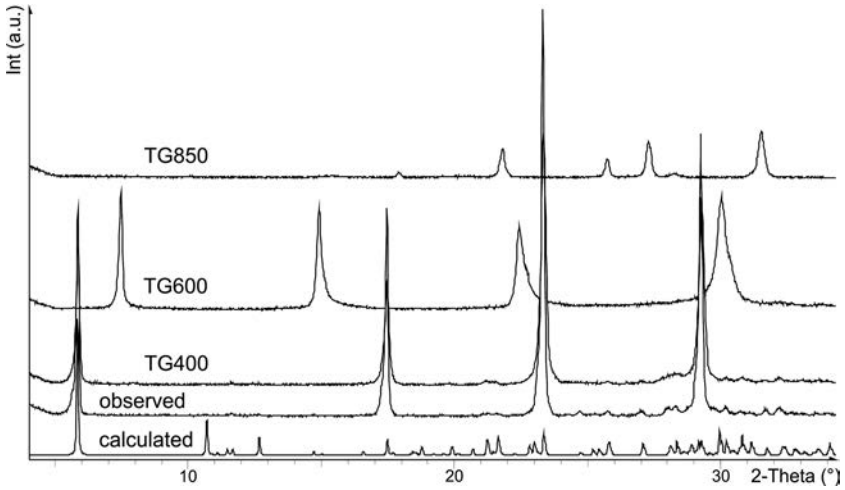

Fig. 3. Cu$K\alpha$ PXRD patterns of cairncrossite, calculated (Kraus & Nolze, 1996), observed with Bragg-Brentano diffractometry and patterns after TG heating up to 400, 600 and 850°C.

Table 1. X-ray powder diffraction data for cairncrossite.

[a] d_{obs} (Å)	[b] d_{cal} (Å)	[a] I_{obs}	[c] I_{cal}	[c] h	k	l
15.230	**15.2277**	**100**	100.0	**0**	**0**	**1**
8.290	**8.2897**	**15**	24.5	**1**	**−1**	**0**
8.280	8.2823	1	3.3	1	0	0
7.730	7.7300	1	5.3	−1	0	1
7.600	7.6007	1	4.4	1	−1	1
7.000	6.9981	10	14.9	−1	1	1
6.030	6.0282	1	3.2	−1	0	2
5.350	5.3520	2	3.6	−1	1	2
5.080	**5.0759**	**25**	15.1	**0**	**0**	**3**
5.020	5.0165	1	1.9	0	1	2
4.729	4.7278	1	4.7	1	1	0
4.533	4.5314	1	1.7	1	−1	3
4.460	4.4606	5	8.4	−1	−1	2
4.294	4.2939	5	6.1	−1	2	1
4.182	4.1826	5	15.9	0	−2	1
4.110	4.1085	5	9.1	−2	1	2
4.100	4.1027	5	11.1	2	−2	1
4.088	4.0874	1	1.2	1	0	3
3.894	3.8937	5	8.0	−1	−1	3
3.865	3.8650	5	9.6	−2	0	2
3.807	**3.8069**	**30**	21.1	**0**	**0**	**4**
3.597	3.5960	1	2.7	1	−1	4
3.450	3.4543	5	10.7	2	−1	3
3.290	3.2905	5	10.7	0	2	2
3.175	3.1739	5	4.4	−1	2	3
3.146	3.1443	10	14.3	1	1	3
3.085	3.0856	5	8.8	1	2	0
3.045	**3.0455**	**20**	11.8	**0**	**0**	**5**
2.978	2.9784	10	25.2	−3	1	2
2.955	2.9541	10	8.3	2	−1	4
2.900	2.8998	5	17.7	1	2	1
2.866	2.8664	1	13.5	2	−3	3
2.815	2.8155	1	7.5	1	−2	5
2.763	2.7630	5	5.0	0	−2	5
2.730	2.7293	1	6.1	−2	3	2
2.700	2.6998	1	2.7	1	1	4
2.659	2.6590	5	4.9	1	2	2
2.625	2.6254	5	11.6	2	−3	4
2.538	2.5379	1	1.6	0	0	6
2.508	2.5081	5	5.9	−3	1	4
2.463	2.4633	10	5.3	−1	−1	6
2.395	2.3950	1	2.6	−3	0	4
2.347	2.3468	1	1.7	−2	2	5
2.308	2.3083	1	1.5	2	0	5
2.265	2.2655	5	1.8	−2	1	6
2.238	2.2381	1	2.5	−2	3	4
2.207	2.2077	1	2.0	0	2	5
2.042	2.0425	1	3.0	−3	1	6
1.958	1.9585	5	3.8	1	2	5
1.896	1.8962	5	0.6	1	−1	8
1.824	1.8237	10	9.6	−4	−1	1
1.815	1.8147	10	6.4	−5	4	0
1.755	1.7546	5	5.0	2	−3	8
1.523	1.5228	5	2.3	0	0	10

Measurement conditions: Gandolfi camera, Ø 114.59 mm, Cu$K\alpha$, Ni-filtered, 24 h; [a] d_{obs} and I_{obs} estimated visually; [b] d_{cal} from the least-squares refinement with UnitCell-v2006 (Holland & Redfern, 1997); [c] *hkl* assignment based on a theoretical powder pattern calculated with PowderCell-v2000 (Kraus & Nolze, 1996) using cell and structural parameters of the single-crystal structure refinement.

Table 2. Crystal data and details of the intensity measurement and structure refinement for cairncrossite.

Crystal data	
Space group	$P\bar{1}$
a (Å)	9.6265(5)
b (Å)	9.6391(5)
c (Å)	15.6534(10)
α (°)	100.89(1)
β (°)	91.27(1)
γ (°)	119.73(1)
V (Å^3)	1227.08(13)
Z	1
ρ_{calc} ($g.\ cm^{-3}$)	2.486
μ (Mo$K\alpha$) (mm^{-1})	3.36
Data collection and refinement	
Unique data	12943
Data with $F_o > 4\sigma(F_o)$	9132
Variables	430
$R1$ [for $F_o > 4\sigma(F_o)$] [1]	0.047
$wR2$ [for all F_o^2] [1]	0.091
a, b [1]	0.0163, 2.6
$\Delta\rho_{min/max}$ (eÅ^{-3})	−1.04/0.82

[1] $R1 = \Sigma \, ||F_o| - |F_c|| / \Sigma \, |F_o|$; $wR2 = [\Sigma w(F_o^2 - F_c^2)^2 / \Sigma w(F_o^2)^2]^{1/2}$; $w = 1/[\sigma^2(F_o^2) + (a \times P)^2 + b \times P]$; $P = \{[\max \text{ of } (0 \text{ or } F_o^2)] + 2F_c^2\}/3$

omega-scans with 2° scanwidth (total 802 frames, 150 s per frame) were measured at a crystal-detector distance of 35 mm up to 78 °2θ (full sphere complete to 70 °2θ). The absorption was corrected by evaluation of multi-scans. Selected crystal parameters as well as a summary on data collection and structure refinements for the best crystal fragment of cairncrossite, $Sr_2Ca_{7-x}Na_{2x}(Si_4O_{10})_4(OH)_2 \cdot (H_2O)_{15-x}$ (with x close to 1) are given in Table 2. The crystal structure was solved by direct methods (Shelxs97: Sheldrick, 2008) and refined by full-matrix least-squares techniques (Shelxl97: Sheldrick, 2008). Except for disordered H_2O molecules (oxygen atoms OW7a and OW7b), the positions of the hydrogen atoms were located by final difference Fourier maps and refined with idealized geometry. In the structure of cairncrossite, cations are located on one special (Ca1) and four general sites (Sr, Ca2-4). In the initial model, anisotropic displacement parameters (ADP's) for Ca1 and Ca4 indicated partial substitution of calcium by sodium on these positions. A subsequent refinement of the Ca:Na ratio yielded values of ~0.80:0.20 and ~0.60:0.40 for the sites Ca1 and Ca4, respectively, reducing $R1$ from 5.5 to 4.8 %, while the positions Ca2, Ca3 and Sr are fully occupied by Ca and Sr, respectively. To achieve charge balance, the presence of further cations had to be assumed. A residual peak of 5 eÅ^{-3} located close to the origin and refined solely as a disordered H_2O molecule in the first model most probably can be considered to house additional cations, especially sodium and/or calcium. Assuming occupation of this split site (Na5) solely by sodium results in a refined occupation factor of 0.49, which is close to the maximal occupation factor possible. Final atomic positions and main interatomic bond distances and angles are listed in Tables 3

Table 3. Atomic fractional coordinates and displacement parameters with e.s.d.'s in parentheses for cairncrossite. Site symmetries (with Wyckoff positions in parentheses) are 1 (2*i*) for all atoms except $\overline{1}$ for Ca1 (1*h*). The refined Ca/Na ratios are ~ 0.798(2)/0.202(2) and ~ 0.601(1)/0.399(1) for Ca1 and Ca4, respectively. Disordered oxygen atom sites OW7a and OW7b as well as Na5 are half occupied.

	x	*y*	*z*	$U_{iso/eq}$	U_{11}	U_{22}	U_{33}	U_{23}	U_{13}	U_{12}
Sr	0.32058(3)	0.74704(3)	0.00317(2)	0.01862(6)	0.01537(11)	0.01827(11)	0.01463(12)	0.00525(9)	−0.00202(9)	0.00266(9)
Ca1	0.5	0.5	0.5	0.01045(14)	0.0087(3)	0.0095(3)	0.0137(3)	0.0036(3)	0.0024(2)	0.0047(2)
Ca2	0.20882(5)	0.64463(5)	0.49487(3)	0.00903(8)	0.00805(17)	0.00744(16)	0.0111(2)	0.00273(15)	0.00097(15)	0.00337(14)
Ca3	0.36022(5)	0.08219(5)	0.52060(3)	0.00936(8)	0.00700(17)	0.00719(17)	0.0135(2)	0.00274(15)	0.00185(15)	0.00322(14)
Ca4	0.07830(7)	0.21750(7)	0.50569(4)	0.01284(12)	0.0123(3)	0.0133(2)	0.0153(3)	0.0058(2)	0.0037(2)	0.0075(2)
Na5	0.0053(10)	0.0675(12)	0.0088(6)	0.138(4)	0.089(4)	0.269(14)	0.125(5)	0.130(9)	0.056(4)	0.113(7)
Si1	0.38637(7)	0.54438(7)	0.31313(4)	0.00711(11)	0.0044(2)	0.0075(2)	0.0087(3)	0.0027(2)	0.0012(2)	0.00220(19)
Si2	0.01990(7)	0.30527(7)	0.31822(4)	0.00662(11)	0.0053(2)	0.0053(2)	0.0089(3)	0.0024(2)	0.0007(2)	0.00214(19)
Si3	0.89597(7)	0.93291(7)	0.31419(4)	0.00729(11)	0.0060(2)	0.0069(2)	0.0100(3)	0.0032(2)	0.0014(2)	0.0036(2)
Si4	0.14449(7)	0.81765(7)	0.32769(4)	0.00682(11)	0.0052(2)	0.0056(2)	0.0092(3)	0.0016(2)	0.0001(2)	0.00252(19)
Si5	0.51036(7)	0.05752(7)	0.32791(4)	0.00740(11)	0.0056(2)	0.0054(2)	0.0111(3)	0.0027(2)	0.0017(2)	0.00240(19)
Si6	0.63459(7)	0.41804(7)	0.32231(4)	0.00807(11)	0.0080(3)	0.0083(2)	0.0105(3)	0.0046(2)	0.0035(2)	0.0051(2)
Si7	0.57694(7)	0.80560(7)	0.21021(4)	0.00756(11)	0.0056(2)	0.0073(2)	0.0091(3)	0.0031(2)	0.0006(2)	0.0024(2)
Si8	0.91029(7)	0.47584(7)	0.21859(4)	0.00737(11)	0.0067(2)	0.0066(2)	0.0084(3)	0.0020(2)	0.0007(2)	0.0030(2)
O1	0.4220(2)	0.6513(2)	0.41065(12)	0.0156(4)	0.0129(8)	0.0155(8)	0.0110(8)	−0.0007(6)	0.0021(6)	0.0029(6)
O2	0.1990(2)	0.4003(2)	0.28912(12)	0.0130(3)	0.0072(7)	0.0121(7)	0.0164(9)	0.0035(6)	0.0020(6)	0.0024(6)
O3	0.4890(2)	0.4516(2)	0.30522(14)	0.0180(4)	0.0145(8)	0.0195(8)	0.0289(11)	0.0108(8)	0.0064(7)	0.0132(7)
O4	0.4271(2)	0.6452(2)	0.23585(12)	0.0125(3)	0.0093(7)	0.0126(7)	0.0137(8)	0.0081(6)	0.0013(6)	0.0025(6)
O5	0.5508(2)	0.8013(3)	0.11019(13)	0.0262(5)	0.0163(9)	0.0340(11)	0.0142(9)	0.0150(8)	−0.0027(7)	−0.0004(8)
O6	0.7421(2)	0.8093(2)	0.23973(13)	0.0156(4)	0.0085(7)	0.0097(7)	0.0262(10)	−0.0027(7)	−0.0052(7)	0.0054(6)
O7	0.5957(2)	0.9688(2)	0.27386(17)	0.0275(5)	0.0128(8)	0.0131(8)	0.0510(15)	−0.0051(9)	0.0100(9)	0.0065(7)
O8	0.8583(3)	0.9338(3)	0.41234(13)	0.0247(5)	0.0238(10)	0.0515(14)	0.0169(10)	0.0191(10)	0.0123(8)	0.0283(10)
O9	−0.0259(2)	0.1160(2)	0.29755(13)	0.0159(4)	0.0134(8)	0.0063(7)	0.0269(10)	0.0051(7)	0.0012(7)	0.0039(6)
O10	0.0287(2)	0.8790(2)	0.29420(12)	0.0128(3)	0.0117(7)	0.0150(7)	0.0172(9)	0.0043(7)	0.0012(6)	0.0106(6)
O11	0.1553(2)	0.8217(2)	0.43014(11)	0.0105(3)	0.0108(7)	0.0109(7)	0.0093(8)	0.0036(6)	0.0013(6)	0.0047(6)
O12	0.0791(2)	0.6334(2)	0.27075(12)	0.0130(3)	0.0114(7)	0.0072(7)	0.0185(9)	−0.0019(6)	−0.0027(6)	0.0051(6)
O13	0.31853(19)	0.9371(2)	0.30097(12)	0.0131(3)	0.0055(7)	0.0132(7)	0.0158(9)	0.0042(6)	0.0013(6)	0.0010(6)
O14	0.9030(2)	0.4549(2)	0.11600(11)	0.0140(3)	0.0133(8)	0.0167(8)	0.0090(8)	0.0029(6)	0.0016(6)	0.0055(6)
O15	0.7605(2)	0.4941(2)	0.25376(12)	0.0129(3)	0.0129(7)	0.0130(7)	0.0179(9)	0.0094(7)	0.0083(6)	0.0083(6)
O16	0.9008(2)	0.31739(19)	0.24838(12)	0.0114(3)	0.0093(7)	0.0082(7)	0.0151(8)	0.0023(6)	−0.0036(6)	0.0036(6)
O17	0.7130(2)	0.4916(2)	0.42258(12)	0.0141(3)	0.0186(8)	0.0153(8)	0.0111(8)	0.0034(6)	0.0024(7)	0.0104(7)
O18	0.5559(2)	0.2203(2)	0.29248(12)	0.0135(3)	0.0174(8)	0.0080(7)	0.0160(9)	0.0062(6)	0.0045(7)	0.0058(6)
O19	0.5672(2)	0.0982(2)	0.43063(12)	0.0131(3)	0.0120(7)	0.0110(7)	0.0127(8)	0.0042(6)	–0.0022(6)	0.0029(6)
O20	0.0110(2)	0.3729(2)	0.41812(11)	0.0130(3)	0.0125(7)	0.0142(7)	0.0086(8)	0.0010(6)	0.0016(6)	0.0047(6)
O_H1	0.3004(2)	0.2333(2)	0.44137(13)	0.0145(3)	0.0055(7)	0.0132(7)	0.0158(9)	0.0042(6)	0.0013(6)	0.0010(6)
H	0.286(5)	0.206(5)	0.389(2)	0.044(13)						
O_W1	0.5438(3)	0.9304(3)	–0.09284(17)	0.0363(6)	0.0416(15)	0.0330(13)	0.0223(12)	0.0064(10)	0.0049(10)	0.0102(11)
H1a	0.598(6)	0.899(6)	–0.116(3)	0.054						
H1b	0.494(6)	0.921(6)	–0.140(3)	0.054						
O_W2	0.1932(3)	0.5007(3)	0.07945(14)	0.0235(4)	0.0156(9)	0.0315(11)	0.0193(10)	0.0062(9)	0.0022(8)	0.0089(8)
H2a	0.253(5)	0.536(5)	0.127(2)	0.035						
H2b	0.102(4)	0.477(5)	0.091(3)	0.035						

O_w3	0.2153(3)	0.9121(3)	–0.07596(17)	0.0384(6)	0.0464(15)	0.0200(11)	0.0283(13)	0.0084(10)	–0.0053(11)	0.0014(10)
H3a	0.292(5)	1.009(5)	–0.086(3)	0.058						
H3b	0.185(6)	0.857(6)	–0.126(2)	0.058						
O_w4	0.0888(3)	0.7571(3)	0.08128(19)	0.0386(6)	0.0458(15)	0.0286(12)	0.0386(15)	0.0138(11)	0.0209(12)	0.0142(12)
H4a	0.029(5)	0.671(5)	0.095(3)	0.058						
H4b	0.086(6)	0.825(5)	0.119(3)	0.058						
O_w5	0.4180(4)	0.5561(4)	–0.08361(19)	0.0447(7)	0.0443(16)	0.0643(19)	0.0308(14)	0.0036(14)	–0.0010(13)	0.0344(16)
H5a	0.510(5)	0.579(7)	–0.083(4)	0.067						
H5b	0.374(6)	0.517(6)	–0.138(3)	0.067						
O_w6	0.1871(6)	0.1022(5)	0.1464(3)	0.0751(12)	0.108(3)	0.064(2)	0.061(2)	0.0104(19)	0.032(2)	0.050(2)
H6a	0.185(8)	0.163(7)	0.201(3)	0.113						
H6b	0.263(7)	0.187(7)	0.125(4)	0.113						
O_w7a	0.2682(10)	0.2725(13)	–0.0006(8)	0.050(2)	0.050(5)	0.050(5)	0.055(5)	0.007(4)	–0.001(4)	0.031(4)
O_w7b	0.1958(12)	0.2258(14)	–0.0158(9)	0.065(3)	0.080(7)	0.054(6)	0.070(7)	0.006(5)	0.018(7)	0.043(6)

and 4, respectively. Details on the hydrogen bond system are summarized in Table 5.

Raman spectroscopy

Raman microprobe measurements were done on a Renishaw RM1000 Raman spectrometer with 488 nm Ar laser excitation (8 mW measured behind the microscope objective). An Olympus 50× objective (n.a. 0.55) was used. Raman-shift calibration, done using the Rayleigh line and Ne lamps emissions, ensured that the wavenumber accuracy was better than 1 cm^{-1}. The spectral resolution was ~5–6 cm^{-1}. To reach a sufficient signal/noise ratio, all spectra were acquired for 120 s.

The Raman spectrum of cairncrossite (Fig. 4a) is characterized by two sharp peaks at 610 and 1060 cm^{-1}. The band at 1060 cm^{-1} is due to the Si–O stretching vibration, the band at 610 cm^{-1} to the Si–O bending vibration. The bands observed at 3650 and 3670 cm^{-1} are assigned to the stretching vibrations of the OH groups, the broad band centred around 3550 cm^{-1} to stretching vibrations of the H_2O molecules. Considering the correlation diagram of Libowitzky (1999), the position of this band indicates mean O-H…O distances of ~ 2.95 A which is in good agreement with the hydrogen bonds observed (Table 5). The spectrum of the new mineral cairncrossite is similar to that of gyrolite (*cf.* Fig. 4b).

Discussion

Description of the crystal structure

The crystal structure of cairncrossite (see Fig. 5) described as follows is based on the structure refinement of a sodium-rich fragment with the approximate formula $SrCa_3Na(Si_4O_{10})_2(OH)(H_2O)_7$. It is characterized by sheets consisting of edge-sharing CaO_6 octahedra, which are corner-linked on both sides to silicate layers. These units are intercalated by layers formed by SrO_8 polyhedra, which are arranged in pairs via a common edge, and further bound to disordered NaO_6 polyhedra. A complex system of hydrogen bonds strengthens the linkage to the adjacent silicate layers.

Four types of "CaO_6 octahedra", $Ca(1)O_4(OH)_2$ on a centre of symmetry, and further $Ca(2)O_6$ as well as $Ca(3,4)O_5(OH)$ at general positions, share common edges to build sheets parallel (001), as illustrated in Fig. 6. While Ca2 and Ca3 are fully occupied by calcium atoms within the limits of error, Ca1 and Ca4 are significantly substituted by sodium atoms with refined Ca/Na ratios of ~ 0.80/0.20 and ~ 0.60/0.40, respectively. Mean $Ca^{[6]}$–O bond lengths are 2.407 and 2.380 Å for Ca2 and Ca3, but somewhat larger for mixed sites Ca1 (2.424 Å) and Ca4 (2.447 Å). Calculated bond strengths (according to Brese & O'Keeffe, 1991) yield values of 1.81, 1.84, 1.97 and 1.69 valence units (v.u.) for Ca1-4. Oxygen ligands of the CaO_6

Table 4. Selected interatomic bond distances [Å] and angles (°) for cairncrossite. E.s.d.'s for O-Si-O angles are ~ 0.1°.

Sr–	O14	2.4888(18)	Si1–	O1	1.5942(19)	
	O5	2.519(2)		O2	1.6163(17)	
	O_W4	2.602(3)		O3	1.6217(19)	
	O_W2	2.611(2)		O4	1.6274(17)	
	O_W5	2.633(3)	<Si1–O>	O-Si1-O	1.615	105.6–115.7
	O_W3	2.716(3)				
	O_W1	2.717(3)	Si2–	O20	1.5980(18)	
	O_W1	2.754(3)		O9	1.6127(18)	
<Sr–O>		2.630		O2	1.6261(17)	
				O16	1.6278(18)	
Ca1–	O_H1 2×	2.2968(19)	<Si2–O>	O-Si2-O	1.616	103.6–114.0
	O17 2×	2.4328(18)				
	O1 2×	2.5411(19)	Si3–	O8	1.586(2)	
<Ca1–O>		2.424		O9	1.6167(17)	
				O10	1.6179(18)	
Ca2–	O17	2.3531(18)		O6	1.6189(19)	
	O19	2.3764(18)	<Si3–O>	O-Si3-O	1.610	105.5–114.9
	O20	2.3861(18)				
	O11	2.3888(17)	Si4–	O11	1.5967(18)	
	O1	2.4445(19)		O13	1.6148(17)	
	O20	2.4945(18)		O10	1.6155(18)	
<Ca2–O>		2.407		O12	1.6164(18)	
			<Si4–O>	O-Si4-O	1.611	104.5–114.7
Ca3–	O8	2.3213(19)				
	O_H1	2.3395(19)	Si5–	O19	1.5965(19)	
	O1	2.3802(18)		O7	1.605(2)	
	O19	2.4035(18)		O13	1.6092(17)	
	O11	2.4128(17)		O18	1.6183(17)	
	O19	2.4250(19)	<Si5–O>	O-Si5-O	1.607	106.1–113.3
<Ca3–O>		2.380				
			Si6–	O17	1.5913(19)	
Ca4–	O_H1	2.3321(19)		O3	1.6148(19)	
	O11	2.3685(18)		O15	1.6223(17)	
	O8	2.387(2)		O18	1.6250(18)	
	O20	2.4979(19)	<Si6–O>	O-Si6-O	1.613	105.9–113.9
	O17	2.5066(19)				
	O8	2.590(3)	Si7–	O5	1.570(2)	
<Ca4–O>		2.447		O7	1.618(2)	
				O6	1.6266(19)	
Na5–	Ow7a	2.344(13)		O4	1.6375(17)	
	O_W3	2.468(7)	<Si7–O>	O-Si7-O	1.613	103.6–113.4
	Ow7b	2.540(15)				
	O_W6	2.607(9)	Si8–	O14	1.5757(18)	
	O_W6	2.703(11)		O12	1.6246(18)	
	O_W4	2.834(6)		O15	1.6316(18)	
				O16	1.6403(17)	
			<Si8–O>	O-Si8-O	1.618	105.3–112.2

octahedra belong either to a hydroxyl group or are part of SiO_4 tetrahedra.

Eight different SiO_4 tetrahedra are present in the structure of cairncrossite, forming a silicate layer $[Si_4O_{10}]^{4-}$ composed of six-membered rings. This layer is corner-connected via $Si(1–6)O_4$ tetrahedra (Figs. 5 and 6) to the sheet of CaO_6 octahedra and via $Si(7,8)O_4$ tetrahedra (Fig. 7) to the SrO_8 groups. Mean Si–O distances are between 1.607 and 1.618 Å, somewhat short but well in the range reported for silicate tetrahedra (Liebau, 1985). Respective bond valence sums are 4.07–4.19 v.u. Bond length distortions are moderate, the respective shortest Si–O bond belongs to the apex corner-linked to neighbouring sheets of CaO_6 or SrO_8 groups.

These SrO_8 groups, more explicitly $SrO_2(O_w)_6$, distorted tetragonal antiprisms, are arranged in pairs sharing one common edge O_w1–O_w1 (Fig. 8). The mean $Sr^{[8]}$–O bond length is 2.630 Å and the bond-valence sum amounts to 2.06 v.u. Minor amounts of potassium detected by microprobe most likely substitute strontium at this site.

Assuming partial substitution of Ca by Na on Ca1 and Ca4 to an extent as reported above, one additional positive charge per unit cell is necessary to achieve charge balance, resulting in a replacement "$Ca_{7-x}Na_{2x}$". The most plausible explanation is the presence of further cations on a disordered position close to the origin. A cation, strictly located at this centre of symmetry, would be 6-coordinated to H_2O molecules O_w7, O_w6 and O_w3 with a mean bond

Table 5. Hydrogen bonding scheme (Å, °) for cairncrossite.

D	H	D–H	A	D···A	D–H···A	H-D-H
O_W1–	H1a	0.79(4)	Ow6	2.883(5)	158(5)	
	H1b	0.84(4)	O18	3.093(3)	138(4)	
						94(5)
O_W2–	H2a	0.83(3)	O14	2.696(3)	172(4)	
	H2b	0.83(3)	O4	2.891(3)	172(4)	
						108(4)
O_W3–	H3a	0.90(4)	O5	2.726(3)	177(5)	
	H3b	0.81(4)	O16	2.930(3)	172(5)	
						100(4)
O_W4–	H4a	0.81(4)	O14	2.730(3)	171(5)	
	H4b	0.81(4)	Ow6	2.922(5)	136(5)	
						103(5)
O_W5–	H5a	0.80(4)	Ow7a	2.764(8)	140(5)	
	H5b	0.87(4)	O15	2.961(3)	154(5)	
						107(5)
O_W6–	H6a	0.94(4)	O2	3.242(4)	158(6)	
	H6b	0.92(4)	Ow7a	2.972	134(6)	99(4)
O_H–	H	0.80(3)				

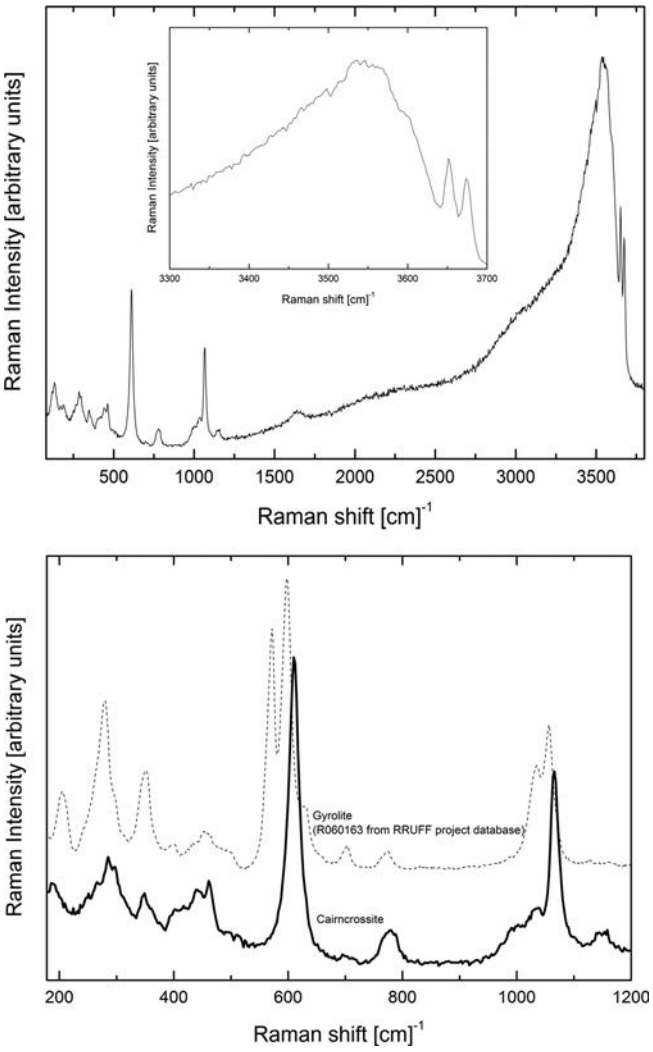

Fig. 4. (a) Raman spectrum of cairncrossite and (b) detail of the spectrum as compared to that of gyrolite.

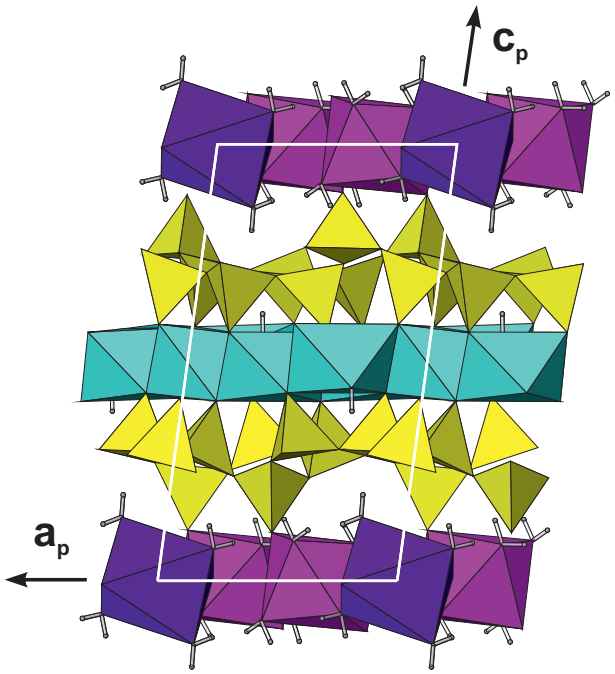

Fig. 5. Crystal structure overview of cairncrossite, projected along [010]. The CaO_6 octahedra are indicated in light blue shades, SiO_4 tetrahedra in yellow, SrO_8 polyhedra in magenta and the idealized NaO_6 octahedron (at origin for an unsplit sodium atom) in purple. All figures of crystal structures were created with the program ATOMS (Dowty, 2013).

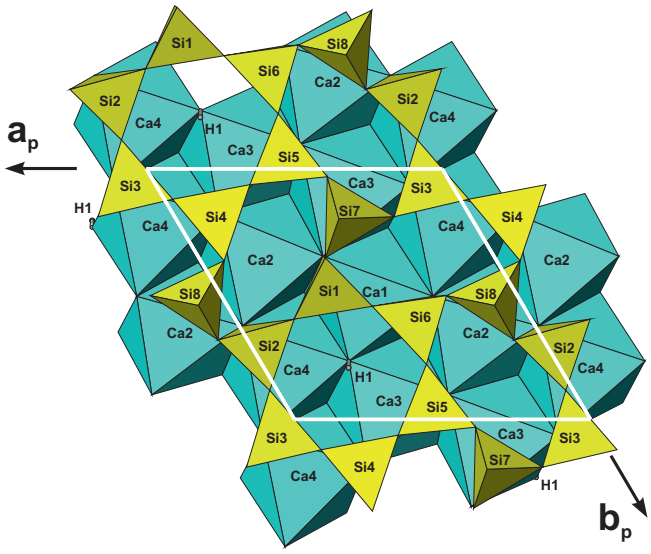

Fig. 6. Detail of the crystal structure, projected along [001]. A single layer composed of CaO_6 octahedra, centred around $z/c = 0.5$, is shown, as linked to the silicate rings above. (online version in colour)

distance of ~ 2.58 Å. In Figs. 5 and 7 this simplified model is used to illustrate the coordination around Na5. Based on electron-density maps, it is evident that this site (Na5) is split into two half-occupied positions, separated from each other by 1.23 Å. Furthermore, one H_2O ligand (O_w7) is split, too, with a O_w7a–O_w7b distance of 0.62 Å.

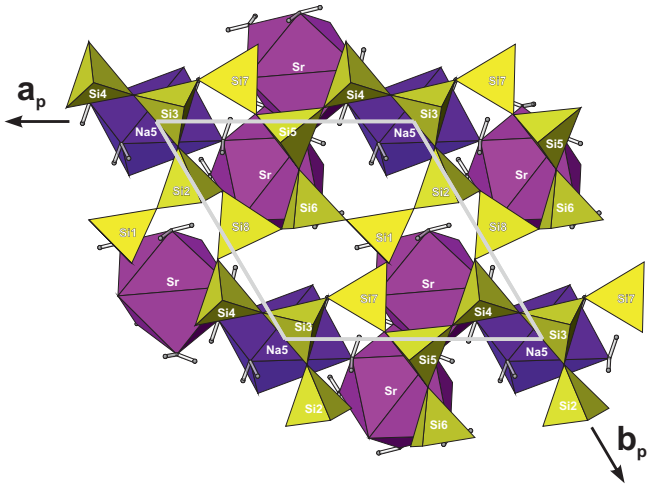

Fig. 7. Detail of the crystal structure at height z/c = 0.0, projected along [001]. The interlayer is composed of edge-sharing pairs of SrO_8 polyhedra, corner-linked to the idealized NaO_6 octahedron. The silicate sheet above is further shown.

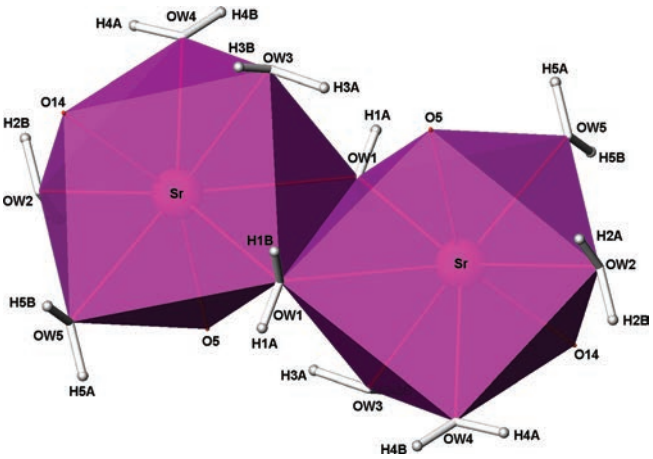

Fig. 8. The $Sr_2O_4(O_w)_{10}$ unit in cairncrossite.

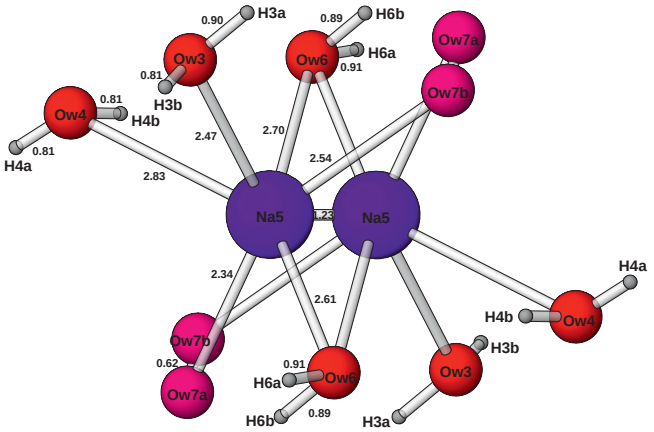

Fig. 9. Ball-and-stick model illustrating the coordination around the split Na5 cation. Positions of hydrogen atoms belonging to the disordered O_w7a,b atoms could not be located.

According to this model shown in Fig. 9, the local six-fold coordination around the split cation is modified as listed in Table 4, involving O_w4. Comfortingly, the mean $Na^{[6]}$–O distance is reduced to 2.53 Å to accommodate space requirements of sodium; the sum of bond valences is 0.79 v.u. Similar $Na^{[6]}$–O distances have been observed, *e.g.*, in the rare zeolite nabesite (Petersen *et al.*, 2002).

Oxygen atoms of cairncrossite can be categorized as follows:

Ia) Shared ligands of two Si atoms (oxygens no. 2–4, 6, 7, 9, 10, 12, 13, 15, 16 and 18). The Si-O-Si angles range between 131.3 and 159.8°, calculated bond strengths between 1.95 and 2.07 v.u.

Ib) Oxygen atoms bound to one Si and one Sr atom (oxygens no. 5 and 14). The Si-O-Sr angles are 135.9 and 129.9°, calculated bond strengths are 1.50 and 1.51 v.u., respectively. These two oxygen atoms function as acceptors for the strongest hydrogen bonds observed in cairncrossite.

Ic) Oxygen atoms bound to one Si and three Ca atoms in a strongly distorted tetrahedral arrangement (oxygens no. 1, 8, 11, 17, 19 and 20). Calculated bond strengths are between 1.87 and 2.03 v.u.

II) Oxygen O_H1, belonging to a hydroxyl group. O_H1 is coordinated to three calcium atoms and the hydrogen atom H1 in a fairly regular tetrahedral coordination. The calculated bond strength (without contribution of H1) is 1.15 v.u. The hydrogen atom, pointing towards the centre of a neighbouring six-membered silicate ring (Fig. 6), is not involved in hydrogen bonding.

IIIa) Oxygen atoms of H_2O molecules, further bound to two cations (Sr and/or Na5) in distorted tetrahedral coordination (oxygens O_w1, O_w3, O_w4 and O_w6). The calculated bond strengths (without taking hydrogens into account) are 0.20–0.38 v.u.

IIIb) Oxygen atoms of H_2O molecules, further bound to one cation (Sr or Na5) in non-planar coordination (oxygens O_w2, O_w5, and the split, half-occupied atoms O_w7a and O_w7b). Respective bond strengths range from 0.14 to 0.26 v.u.

The proposed hydrogen bonding scheme in cairncrossite, based on approximate location of hydrogen atoms from the refinement and on estimation of bond strengths, is listed in Table 5. Donor-acceptor distances span a wide range from ~ 2.7 Å up to far more than 3.0 Å for weak contributions.

Related species

Cairncrossite belongs to the gyrolite–reyerite mineral groups (see subdivision 9.EE30-35 of the Strunz Mineralogical Tables, Strunz & Nickel, 2001). These phyllosilicates all show six-membered rings of silicate tetrahedra which are bound to sheets composed of edge-sharing CaO_6 octahedra. Intercalated between these complex units,

a variety of further cations, commonly hydrated, are found. Calcium, abundant in this group of minerals, is commonly partially substituted by other cations, especially sodium and potassium, as also observed in cairncrossite. Representatives are either trigonal, or triclinic with distorted pseudotrigonal unit cells (with *a* and *b* ranging from 9.6 to 9.8 Å but strongly differing in *c*, due to the respective stacking of layers).

McDonald & Chao (2009) described the occurrence and crystal structure of a further representative, lalondeite, a hydrated Na-Ca fluorosilicate from Mont Saint-Hilaire. In that article, an overview of the gyrolite and reyerite groups is presented. The structure arrangement in lalondeite $(Na,Ca)_6(Ca,Na)_3Si_{16}O_{38}(F,OH)_2(H_2O)_3$ (*cf.* Fig. 3 in McDonald & Chao, 2009) and cairncrossite is remarkably similar (*e.g.* in respect of polyhedral linkage, cation substitution, bond distances). The main difference is found with respect to the silicate layers which share common corners in lalondeite thus condensing the structure along [001], an atomic arrangement similarly known from fedorite $(Na,K)_{2\text{-}3}(Ca_4Na_3)Si_{16}O_{38}(OH,F)_2(H_2O)_{3.5}$ (Mitchell & Burns, 2001). In the complex structure of gyrolite $NaCa_{16}Si_{23}AlO_{60}(OH)_8(H_2O)_{14}$ (Merlino, 1988), one dominant stacking motif resembles cairncrossite, but interlayer polyhedra are isolated without sharing common edges.

Acknowledgements: The authors thank the reviewers and the editorial team for valuable comments.

References

Bartelmehs, K.L., Bloss, F.D., Downs, R.T., Birch, J.B. (1992): EXCALIBR II. *Z. Kristallogr.*, **199**, 185–196.

Brese, N.E. & O'Keeffe, M. (1991): Bond-valence parameters for solids. *Acta Crystallogr.*, **B47**, 192–197.

Dowty, E. (2013): Atoms V6.4.1 for atomic structure display. Shape Software, 521 Hidden Valley Road, Kingsport, TN 37663 USA.

Gandolfi, G. (1964): Metodo per ottenere uno spettro di polveri da un cristallo singolo di piccole dimensioni (fino a 30 μ). *Mineral. Petrogr. Acta*, **10**, 149–156.

Gard, J.A., Luke, K., Taylor, H.F.W. (1981): $Ca_7Si_{16}O_{40}H_2$, a new calcium silicate hydrate phase of the truscottite group. *Cem. Concr. Res.*, **11**, 659–664.

Giester, G. & Rieck, B. (1994): Effenbergerite, $BaCu[Si_4O_{10}]$, a new mineral from the Kalahari Manganese Field, South Africa: description and crystal structure. *Mineral. Mag.*, **58**, 663–670.

Giester, G. & Rieck, B. (1996): Wesselsite, $SrCu[Si_4O_{10}]$, a further new gillespite-group mineral from the Kalahari Manganese Field, South Africa. *Mineral. Mag.*, **60**, 795–798.

Gladstone, J.H. & Dale, T.P. (1863): Researches on the refraction, dispersion, and sensitiveness of liquids. *Phil. Trans. R. Soc. London*, **153**, 317–343.

Holland, T.J.B. & Redfern, S.A.T. (1997): Unit cell refinement from powder diffraction data: the use of regression diagnostics. *Mineral. Mag.*, **61**, 65–77.

Kraus, W. & Nolze, G. (1996): *POWDER CELL* – a program for the representation and manipulation of crystal structures and calculation of the resulting X-ray powder patter. *J. Appl. Crystallogr.*, **29**, 301–303.

Libowitzky, E. (1999): Correlation of O-H stretching frequencies and O-H · · · O hydrogen bond lengths in minerals. *Mh. Chemie*, **130**, 1047–1059.

Liebau, F. (1985): Structural Chemistry of Silicates. Structure, Bonding, and Classification. Springer-Verlag Berlin, Heidelberg, New York, Tokyo 1985. 347 p, ISBN 3-540-1374-5.

Mandarino, J.A. (1976): The Gladstone-Dale relationship - part I: derivation of new constants. *Can. Mineral.*, **14**, 498–502.

Mandarino, J.A. (1981): The Gladstone-Dale Relationship: Part IV. The compatibility concept and its application. *Can. Mineral.*, **19**, 441–450.

McDonald, A.M. & Chao, G.Y. (2009): Lalondeite, a new hydrated Na-Ca fluorosilicate species from Mont Saint-Hilaire, Quebec: description and crystal structure. *Can. Mineral.*, **47**, 181–191.

Merlino, S. (1988): Gyrolite: its crystal structure and crystal chemistry. *Mineral. Mag.*, **52**, 377–387.

Mitchell, R.H. & Burns, P.C. (2001): The structure of fedorite: a re-appraisal. *Can. Mineral.*, **39**, 769–777.

Petersen, O.V., Giester, G., Brandstätter, F., Niedermayr, G. (2002): Nabesite, $Na_2BeSi_4O_{10} \cdot 4H_2O$, a new mineral species from the Ilímaussaq alkaline complex, South Greenland. *Can. Mineral.*, **40**, 173–181.

Pristacz, H., Giester, G., Rieck, B., Lengauer, C.L. (2013): Thermal behaviour of the new mineral cairncrossite, $Sr_2Ca_7(Si_4O_{10})_4(OH)_2 \cdot 15H_2O$. *Mitt. Österr. Mineral. Ges.*, **159**, 116.

Rieck, B., Pristacz, H., Giester, G. (2015): Colinowensite, $BaCuSi_2O_6$, a new mineral from the Kalahari Manganese Field, South Africa, and new data on wesselsite, $SrCuSi_4O_{10}$. *Mineral. Mag*, 79(7), 1769–1778.

Sheldrick, G.M. (2008): A short history of SHELX. *Acta Crystallogr.*, **A64**, 112–122.

Straumanis, M. & Jevinš, A. (1936): Präzisionsaufnahmen nach dem Verfahren von Debye und Scherrer. II. *Z. Physik.*, **98**, 461–475.

Strunz, H. & Nickel, E.H. (2001): Strunz Mineralogical Tables. Chemical-Structural Mineral Classification System. 9. Edition, ISBN 978-3-510-65188-7, E. Schweizerbart'sche Verlagsbuchhandlung (Nägele und Obermiller), Stuttgart.

Von Bezing, K.L., Dixon, R.D., Pohl, D., Cavallo, G. (1991): The Kalahari manganese field: an update. *Mineral. Rec.*, **22**, 279–297.

Wise, W.S. & Tschernich, R.W. (1975): Cowlesite, a new Ca-zeolite. *Am. Mineral*, **60**, 951–965.

Yamanaka, T. & Mori, H. (1981): The structure and polytypes of α-$CaSiO_3$. *Acta Crystallogr.*, **B37**, 1010–1017.

Received 14 August 2015
Modified version received 6 October 2015
Accepted 1 December 2015